Radiative decays of the spin-3/2 to spin-1/2 doubly heavy baryons in QCD

T. M. Aliev,[1,*] E. Askan,[1,2,†] and A. Ozpineci[1,‡]
[1]Physics Department, Middle East Technical University, 06531 Ankara, Turkey
[2]Physics Department, Ankara University, 06100 Ankara, Turkey

(Received 7 July 2023; accepted 24 August 2023; published 13 September 2023)

The spin-3/2 to spin-1/2 doubly heavy baryon transition magnetic dipole G_M and electric quadrupole G_E form factors are calculated in the framework of the light cone sum rules method. Moreover, the decay widths of corresponding radiative transitions are estimated. Obtained results of magnetic dipole moments G_M and decay widths are compared with the results present in the literature.

DOI: 10.1103/PhysRevD.108.054015

I. INTRODUCTION

The quark model predicts the existence of baryons containing two heavy quarks. The doubly heavy baryons constitute an important and promising system to study the structure of physics of a system containing two heavy quarks as well as for understanding the strong interaction at the nonperturbative domain.

Doubly heavy baryons lie on the focus of theoretical and experimental investigations. Experimentally, the first observation of doubly heavy baryon Ξ_{cc}^{+} was reported by SELEX Collaboration [1]. The existence of its iso doublet partner Ξ_{cc}^{++} state was observed by LHCb Collaboration in the $\Lambda_c^+ K^- \pi^+ \pi^+$ spectrum, with the mass $m_{\Xi_{cc}^{++}} = 3621.40 \pm 0.72 \pm 0.14$ MeV [2]. The mass of Ξ_{cc}^{+} has been updated in [2–5]. In the upgraded experiments planned at LHCb with large data samples additional states predicted by the quark model and new decay channels of doubly heavy baryons may be observed.

The tremendous experimental developments triggered theoretical studies on the physics of doubly heavy baryons. Mainly the theoretical studies are concentrated on studying the mass, electromagnetic properties, and weak decays of doubly heavy baryons. These studies are critical to understanding the flavor structure and dynamics of these baryons. The mass of doubly charmed baryons within different approaches has been studied in many works such as constituent quark model [6–13], Regge phenomenology [14,15], QCD sum rules method [16–21], and relativistic quark model (RQM) [22]. The magnetic moment is another important quantity in studying the inner structure of hadrons. The magnetic moment of doubly charmed baryons within different approaches such as the quark model (QM), chiral perturbation theory (χPT), bag model, effective quark mass scheme (EMS), lattice QCD, and harmonic oscillator model are calculated in [23–28], respectively.

The spin-3/2 to spin-½ doubly heavy baryon transition magnetic moments receive special attention as they probe the inner structure as well as possible deformation of heavy baryons.

In the present work, we calculate the transition magnetic moments of doubly heavy baryons with spin-3/2 to spin-1/2 within the light cone QCD sum rules (LCSR). (More about this method can be found in [29,30].) In this method, the operator product expansion (OPE) is performed over twists of nonlocal operators.

The work is organized as follows. In Sec. II we derive light cone sum rules for the transition magnetic moments of doubly heavy spin-3/2 to spin-1/2 transition. In Sec. III we present our numerical results on magnetic moments of considered transitions. In this section, we also present a comparison of our results with predictions of other approaches.

II. LIGHT CONE SUM RULES FOR MAGNETIC MOMENTS OF DOUBLY HEAVY BARYONS

In this section, we will examine the electromagnetic form factors of $3/2 \to 1/2$ transitions between the double heavy baryons with quark content $QQ'q$. This transition in the presence of the electromagnetic field is described by

$$\Pi^{\mu\nu}(p,q) = i \int d^4x \int d^4y e^{ipx+iqy} \times \langle 0|\mathcal{T}\{\eta_{½}(x) j_{el}^{\nu}(y) \bar{\eta}_{3/2}^{\mu}(0)\}|0\rangle, \quad (1)$$

where j_{el}^{ν} is the electromagnetic current given by

*taliev@metu.edu.tr
†easkan@ankara.edu.tr
‡ozpineci@metu.edu.tr

TABLE I. J^P quantum numbers of doubly heavy Ξ baryons.

State	J^P
Ξ_{QQq}	$1/2^+$
Ξ^*_{QQq}	$3/2^+$
$\Xi_{QQ'q}$	$1/2^+$
$\Xi^*_{QQ'q}$	$3/2^+$
$\Xi'_{QQ'q}$	$1/2^+$

$$j^{\nu}_{el} = \sum_{q'} e_{q'} \bar{q}' \gamma^{\nu} q', \tag{2}$$

where $e_{q'}$ is the charge of the quark q' and the sum over is over all quark flavors. Here $\eta_{1/2}$ and $\eta^{\mu}_{3/2}$ are the interpolating currents of spin-1/2 and spin-3/2 baryons, respectively.

The J^P quantum numbers of doubly heavy baryons are given in Table I. Note that $\Xi'_{QQ'q}$ is antisymmetric under the exchange of heavy quarks whereas the remaining states are symmetric in the flavor space.

$$\eta^{(S)} = \frac{N}{2}\epsilon^{abc}\sum_{k=1}^{2}[(Q^{aT}CA_1^k q^b)A_2^k Q'^c + (Q'^{aT}CA_1^k q^b)A_2^k Q^c]$$

$$\eta^{(A)} = \frac{1}{\sqrt{6}}\epsilon^{abc}\sum_{k=1}^{2}[2(Q^{aT}CA_1^k Q'^b)A_2^k q^c + (Q^{aT}CA_1^k q^b)A_2^k Q'^c - (Q'^{aT}CA_1^k q^b)A_2^k Q^c], \tag{3}$$

where a, b, c are color indices, N is the normalization constant which is equal to $\sqrt{2}$ when $Q \neq Q'$, 1; otherwise, C is the charge conjugation matrix, T is the transposition, $A_1^1 = 1$, $A_1^2 = \beta\gamma_5$, $A_2^1 = \gamma_5$, and $A_2^2 = \beta$, and β is an arbitrary parameter. Superscripts (S) and (A) mean symmetric and antisymmetric interpolating currents with respect to the exchange of heavy quarks.

The interpolating current of doubly heavy baryon with spin-3/2 can be written as

$$\eta^{\mu} = \frac{N}{\sqrt{3}}\epsilon^{abc}[(q^{aT}C\gamma^{\mu}Q^b)Q'^c + (q^{aT}C\gamma^{\mu}Q'^b)Q^c + (Q^{aT}C\gamma^{\mu}Q'^b)q^c], \tag{4}$$

where, again, a, b, c are color indices, N is the normalization constant which is equal to $\sqrt{2}$ when $Q \neq Q'$, 1; otherwise, C is the charge conjugation operator. Note that this interpolating current is symmetric under the exchange of any two quark fields.

By introducing the plane wave electromagnetic background field

$$F_{\mu\nu} = i(\varepsilon^{(\lambda)}_{\nu} q_{\mu} - \varepsilon^{(\lambda)}_{\mu} q_{\nu})e^{iqx} \tag{5}$$

and multiplying the correlation function (1) by $\varepsilon^{(\lambda)}_{\nu}$, it can be rewritten in the following form:

$$\Pi^{\mu\nu}(p,s)\varepsilon^{(\lambda)}_{\nu} = i\int d^4x e^{ipx}\langle 0|\mathcal{T}\{\eta_{1/2}(x)\bar{\eta}^{\mu}_{3/2}(0)\}|0_F\rangle. \tag{6}$$

In Eq. (6) the subscript F indicates that all vacuum expectation values are evaluated in the presence of the background field. It should be noted that the correlation function given in Eq. (1) can be obtained from Eq. (6) by expanding latter in powers of the background field and taking into account only terms linear in $F_{\mu\nu}$, which corresponds to the single photon emission. (More about the background field method can be found in [31,32].)

Now let us derive the sum rules for the $3/2 \to 1/2$ transition form factors. According to the sum rules philosophy, the correlation function Eq. (1) has to be calculated in two different kinematic domains. The hadronic representation of the correlation function can be calculated by inserting a full set of hadrons carrying the same quantum numbers as the interpolating currents $\eta_{1/2}$ and $\eta^{\mu}_{3/2}$ and then separating the contributions of ground states. On the other hand, the correlation function can be calculated in deep Euclidean region, where $p^2 \ll 0$ and $(p+q)^2 \ll 0$ with the help of operator product expansion (OPE). The OPE is performed in terms of photon distribution amplitudes (DAs) of increasing twist.

At the hadronic level, the correlation function Eq. (6) can be written as

$$\Pi^{\mu\nu}\epsilon^{(\lambda)}_{\nu} = \frac{\epsilon^{(\lambda)}_{\nu}\langle 0|\eta_{1/2}|B_2(p,s)\rangle\ \langle B_2(p,s)|j^{\nu}_{el}|B_1(p+q,s')\rangle\ \langle B_1(p+q,s')|\bar{\eta}^{\mu}_{3/2}|0\rangle}{(p^2-m_2^2)((p+q)^2-m_1^2)}, \tag{7}$$

where a sum over hadrons and the continuum is not shown explicitly. The matrix elements in Eq. (7) are defined as

$$\langle 0|\eta_{1/2}|B_{1/2}(p,s)\rangle = \lambda_2 u(p,s),$$
$$\langle B_{3/2}(p+q,s)|\bar{\eta}^{\mu}_{3/2}|0\rangle = \lambda_1 \bar{u}^{\mu}(p+q,s), \tag{8}$$

where u is a Dirac spinor, u^μ is a Rarita-Schwinger spinor, and $\lambda_{1(2)}$ is the residue of the spin-3/2(1/2) doubly heavy baryon.

The matrix element of the electromagnetic current sandwiched between spin-1/2 and spin-3/2 states is parametrized in terms of three form factors in the following way [33,34]:

$$\langle B_{1/2}(p,s)|j^\nu_{el}|B_{3/2}(p+q,s)\rangle = \bar{u}(p,s)\Big[G_1(-g^{\alpha\nu}\not{q}+q^\alpha\gamma^\nu)+G_2\Big(-g^{\alpha\nu}\Big(p+\frac{q}{2}\Big)q+q^\alpha\Big(p+\frac{q}{2}\Big)^\nu\Big) + G_3(q^\alpha q^\nu - q^2 g^{\alpha\nu})\Big]\gamma_5 u_\alpha(p+q,s). \tag{9}$$

The last term which is proportional to G_3 does not contribute to the emission of a real photon. In the problem studied in this work, the emitted photon is a real photon. For this reason, only the values of G_1 and G_2 at $q^2=0$ are needed.

Magnetic dipole (G_E) and electric quadrupole (G_E) moments, which are more directly accessible in experiments, are defined through the form factors G_1 and G_2 as [33,34]

$$G_M = \Big[\frac{3m_1+m_2}{m_1}G_1(0)+(m_1-m_2)G_2(0)\Big]\frac{m_2}{3},$$
$$G_E = (m_1-m_2)\Big[\frac{G_1(0)}{m_1}+G_2(0)\Big]\frac{m_2}{3}, \tag{10}$$

where m_1 and m_2 are masses of spin-3/2 and spin-1/2 doubly heavy baryons, respectively. Performing summation over spins for the Dirac and Rarita-Schwinger spinors via

$$\sum u(p,s)\bar{u}(p,s) = (\not{p}+m)$$
$$\sum u_\alpha(p,s)\bar{u}_\beta(p,s) = (\not{p}+m)\Big[-g_{\alpha\beta}+\frac{1}{3}\gamma_\alpha\gamma_\beta - \frac{2p_\alpha p_\beta}{3m^2}-\frac{p_\alpha\gamma_\beta-p_\beta\gamma_\alpha}{3m}\Big], \tag{11}$$

the phenomenological representation of the correlation function can be obtained. In order to obtain the sum rules for transition form factors, two issues need to be addressed:

(1) Besides the spin-3/2 baryon, the current η_μ can also create a negative parity baryon with spin-1/2 from the vacuum. This negative parity baryon also contributed to the correlation function.
(2) Not all Lorentz structures are independent of each other.

The first problem can be solved in the following way. The matrix element of the current η_μ between vacuum and a spin-1/2 baryon can be written as

$$\langle B_{1/2^-}(p+q,s)|\eta_\mu|0\rangle = A\bar{u}(p+q)\Big[(p+q)_\mu - \frac{m}{4}\gamma_\mu\Big], \tag{12}$$

where the fact that $\eta_\mu\gamma^\mu=0$ is used. Hence, it is seen that the contributions of the spin-1/2 baryons are either $\propto (p+q)_\mu$ or have γ_μ at the right. Other structures do not receive any contribution from these spin-1/2 baryons, and only receive contribution from spin-3/2 baryons. In order to solve the second issue and obtain independent Lorentz structures (following [35]) the Dirac matrices are ordered as $\not{q}\not{p}\gamma_\mu$. With this ordering, the hadronic representation of the correlation function becomes

$$\Pi_{\mu\nu}(p,q)\varepsilon^\nu = e\lambda_2\lambda_1\frac{1}{p^2-m_2^2}\frac{1}{(p+q)^2-m_1^2}\{[\varepsilon_\mu(pq)-(\varepsilon p)q_\mu]\{-2G_1m_1-G_2m_1m_2+G_2(p+q)^2 + [2G_1+G_2(m_2-m_1)]\not{p}+m_2G_2\not{q}-G_2\not{q}\not{p}\}\gamma_5 + [q_\mu\not{\varepsilon}-\varepsilon_\mu\not{q}]\{G_1(p^2+m_1m_2)-G_1(m_1+m_2)\not{p}\}\gamma_5 + 2G_1[\not{\varepsilon}(pq)-\not{q}(\varepsilon p)]q_\mu\gamma_5 - G_1\not{\varepsilon}q\{m+\not{p}\}q_\mu\gamma_5 + \text{other structures with } \gamma^\mu \text{ at the end} + \text{structures which are proportional to } (p+q)^\mu\}. \tag{13}$$

Now let us turn our attention to the calculation of the correlation function from the QCD side. After applying Wick theorem the correlation function given in Eq. (6) becomes

$$\Pi_\mu^S(p) = i\int d^4x e^{ipx}\frac{6}{\sqrt{6}}\langle 0|\{S_{Q'}(x)\gamma_5 \mathrm{Tr}[\gamma_\mu S_Q(x)\tilde{S}_q(x)] - S_Q(x)\tilde{S}_q(x)\gamma_\mu S_{Q'}(x)\gamma_5 - S_q(x)\tilde{S}_Q(x)\gamma_\mu S_{Q'}(x)\gamma_5$$
$$- S_{Q'}(x)\tilde{S}_q(x)\gamma_\mu S_Q(x)\gamma_5 + S_Q(x)\gamma_5\mathrm{Tr}[\tilde{S}_q(x)\gamma_\mu S_{Q'}(x)] + S_q(x)\tilde{S}_{Q'}(x)\gamma_\mu S_Q(x)\gamma_5 + \beta S_{Q'}(x)\mathrm{Tr}[\gamma_\mu S_Q(x)\gamma_5\tilde{S}_q(x)]$$
$$- \beta S_Q(x)\gamma_5\tilde{S}_q(x)\gamma_\mu S_{Q'}(x) - \beta S_q(x)\gamma_5\tilde{S}_Q(x)\gamma_\mu S_{Q'}(x) - \beta S_{Q'}(x)\gamma_5\tilde{S}_q(x)\gamma_\mu S_Q(x) + \beta S_Q(x)\mathrm{Tr}[\tilde{S}_q(x)\gamma_\mu S_{Q'}(x)\gamma_5]$$
$$+ \beta S_q(x)\gamma_5\tilde{S}_{Q'}(x)\gamma_\mu S_Q(x)\}|0\rangle_F,$$
$$\Pi_\mu^A(p) = i\int d^4x e^{ipx}\frac{6}{3\sqrt{2}}\langle 0|\{2S_{Q'}(x)\tilde{S}_Q(x)\gamma_\mu S_q(x)\gamma_5 - \beta S_q(x)\gamma_5\tilde{S}_{Q'}(x)\gamma_\mu S_Q(x)$$
$$+ 2S_Q(x)\tilde{S}_{Q'}(x)\gamma_\mu S_q(x)\gamma_5 + 2S_q(x)\gamma_5\mathrm{Tr}[\tilde{S}_Q(x)\gamma_\mu S_{Q'}(x)] - S_{Q'}(x)\gamma_5\mathrm{Tr}[S_Q(x)\gamma_\mu S_q(x)] - S_Q(x)\tilde{S}_q(x)\gamma_\mu S_{Q'}(x)\gamma_5$$
$$- S_q(x)\tilde{S}_Q(x)\gamma_\mu S_{Q'}(x)\gamma_5 + S_{Q'}(x)\tilde{S}_q(x)\gamma_\mu S_Q(x)\gamma_5 + S_Q(x)\gamma_5\mathrm{Tr}[\tilde{S}_{Q'}(x)\gamma_\mu S_q(x)] - S_q(x)\tilde{S}_{Q'}(x)\gamma_\mu S_Q(x)\gamma_5$$
$$+ 2\beta S_{Q'}(x)\gamma_5\tilde{S}_Q(x)\gamma_\mu S_q(x) - 2\beta S_Q(x)\gamma_5\tilde{S}_{Q'}(x)\gamma_\mu S_q(x) + 2\beta S_q(x)\mathrm{Tr}[\gamma_\mu S_{Q'}(x)\gamma_5\tilde{S}_Q(x)]$$
$$- \beta S_{Q'}(x)\mathrm{Tr}[\gamma_5\tilde{S}_q(x)\gamma_\mu S_Q(x)] - \beta S_Q(x)\gamma_5\tilde{S}_q(x)\gamma_\mu S_{Q'}(x) - \beta S_q(x)\gamma_5\tilde{S}_Q(x)\gamma_\mu S_{Q'}(x)$$
$$+ \beta S_{Q'}(x)\gamma_5\tilde{S}_q(x)\gamma_\mu S_Q(x) + \beta S_Q(x)\mathrm{Tr}[\gamma_5\tilde{S}_{Q'}(x)\gamma_\mu S_q(x)]\}|0\rangle_F, \tag{14}$$

where the superscripts $S(A)$ denotes when symmetric(antisymmetric) interpolating current has been used. In Eq. (14), S_Q and S_q are heavy and light quark propagators. Their expressions in the presence of gluonic and electromagnetic background fields are

$$S_q(x) = \frac{i\not{x}}{2\pi^2x^4} - \frac{i}{16\pi^2x^2}\int_0^1 du\{\bar{u}\not{x}\sigma_{\alpha\beta} + u\sigma_{\alpha\beta}\not{x}\}\{gG^{\alpha\beta}(ux) + e_qF^{\alpha\beta}(ux)\}$$
$$S_Q(x) = \frac{m_Q^2}{4\pi^2}\left[\frac{K_1(m_Q\sqrt{-x^2})}{\sqrt{-x^2}} + \frac{i\not{x}}{(\sqrt{-x^2})^2}K_2(m_Q\sqrt{-x^2})\right] - \frac{im_Q}{16\pi^2}\int_0^1 du\{gG^{\alpha\beta}(ux) + e_QF^{\alpha\beta}(ux)\}$$
$$\times\left\{\sigma_{\alpha\beta}K_0(m_Q\sqrt{-x^2}) + \left((\bar{u}\not{x}\sigma_{\alpha\beta} + u\sigma_{\alpha\beta}\not{x})\frac{K_1(m_Q\sqrt{-x^2})}{\sqrt{-x^2}}\right)\right\}, \tag{15}$$

where K_i are the modified Bessel functions of the second kind, $G_{\mu\nu}$ and $F_{\mu\nu}$ are the background gluon and electromagnetic field strength tensors, respectively.

Calculation of the correlation function in the external field involves perturbative and nonperturbative parts; i.e., the photon interacts with the quarks perturbatively or nonperturbatively. To calculate the perturbative part, when the propagators in Eq. (15) are placed in Eq. (14), the terms linear in $F_{\mu\nu}$ are selected. For the calculation of the nonperturbative part, it is enough to replace the light quark propagator that emits the photon with

$$S_q \to -\frac{1}{4}\Gamma_j\bar{q}\Gamma_j q, \tag{16}$$

where $\Gamma_j = \{\mathbf{1}, \gamma_\alpha, i\gamma_5\gamma_\alpha, \gamma_5, \frac{1}{\sqrt{2}}\sigma_{\alpha\beta}\}$. In this case, there are two and three particle matrix elements: $\langle 0|\bar{q}\Gamma_j q|0\rangle_F$, $\langle 0|\bar{q}\Gamma G_{\mu\nu}q|0\rangle_F$, and $\langle 0|\bar{q}\Gamma F_{\mu\nu}q|0\rangle_F$, which are parametrized in terms of photon DAs and describes the interaction of photons with quark fields at large distance.

We see that the hadronic and QCD sides of the correlation function contain many structures. Among all structures, the structures $\not{\epsilon}\not{p}\gamma_5 q_\mu$ and $q\not{p}\gamma_5(\varepsilon p)q_\mu$ exhibit the best convergence; for this reason, we chose them for determination of $G_1(0)$ and $G_2(0)$, respectively. Equating the coefficients of the aforementioned structures on both sides, we get the sum rules for $G_1(0)$ and $G_2(0)$. In the final step, we perform Borel transformation over variables $-p^2$ and $-(p+q)^2$ in order to suppress the higher states and continuum contributions and enhance ground states to obtain

$$(m_2+m_1)G_1(0)\lambda_1\lambda_2 e^{-m_2^2/M_1^2}e^{-m_1^2/M_2^2} + \cdots = \int ds_1\int ds_2 e^{-s_1/M_1^2 - s_2/M_2^2}\rho_1(s_1,s_2),$$
$$G_2(0)\lambda_1\lambda_2 e^{-m_2^2/M_1^2}e^{-m_1^2/M_2^2} + \cdots = \int ds_1\int ds_2 e^{-s_1/M_1^2 - s_2/M_2^2}\rho_2(s_1,s_2), \tag{17}$$

where λ_1 and λ_2 are the residues of the spin-3/2 and spin-1/2 baryons, respectively, and $\cdots$ denotes the contribution from higher states and the continuum. To obtain the sum rules for the form factors G_1 and G_2, the contributions of the higher states and the continuum are subtracted using quark hadron duality:

$$\rho(s_1,s_2) \simeq \rho^{OPE}(s_1,s_2) \quad \text{if } (s_1,s_2) \notin \mathcal{D}, \tag{18}$$

where $\mathcal{D}$ is a domain in the (s_1,s_2) plane. Typically, the domain $\mathcal{D}$ is a rectangular region defined by $s_1 < s_{10}$ and $s_2 < s_{20}$ for some constants s_{10} and s_{20}, or a triangular region. In this work, for its simplicity, continuum subtraction is carried out by choosing $\mathcal{D}$ as the region defined as $s \equiv s_1 u_0 + s_2 \bar{u}_0 < s_0$, where $u_0 \equiv \frac{M_2^2}{M_1^2+M_2^2}$ and $\bar{u}_0 = 1 - u_0$. Introducing a second variable $u = \frac{s_1 u_0}{s}$, the integral in the (s_1,s_2) plane can be written as

$$\int ds_1 \int ds_2 e^{-s_1/M_1^2 - s_2/M_2^2} \rho(s_1,s_2) = \int ds e^{-\frac{s}{M^2}} \rho(s), \tag{19}$$

where

$$\rho(s) = \frac{s}{u_0 \bar{u}_0} \int_0^1 du \rho\left(s\frac{u}{u_0}, s\frac{\bar{u}}{\bar{u}_0}\right). \tag{20}$$

In the problem under study, the masses of the initial and final state baryons are very close to each other; hence, we can set $M_1^2 = M_2^2 = 2M^2$ leading to $u_0 = ½$. Using quark hadron duality, sum rules for the form factors take the form

$$\begin{aligned}(m_1+m_2) G_1(0) \lambda_1 \lambda_2 e^{-m^2/M^2} &= \int_0^{s_0} ds e^{-s/M^2} \rho_1(s), \\ G_2(0) \lambda_1 \lambda_2 e^{-m^2/M^2} &= \int_0^{s_0} ds e^{-s/M^2} \rho_2(s),\end{aligned} \tag{21}$$

where $m^2 = (m_1^2 + m_2^2)/2$ and the expressions of spectral densities $\rho_1(s)$ and $\rho_2(s)$ are presented in the Appendix. Note that although the limits of the s integral are written from $s = 0$ up to $s = s_0$, $\rho_i(s) = 0$ $(i = 1$ or $2)$ for $s < (m_Q + m_{Q'})^2$. From Eq. (21) it follows that, for determination of $G_1(0)$ and $G_2(0)$, the residues λ_1 and λ_2 are needed. Spin-1/2 residues are calculated in [20], while the values for the spin-3/2 residues are calculated in [21].

III. NUMERICAL ANALYSIS

This section is devoted to the analysis of the sum rules for the transition form factors $G_1(0)$ and $G_2(0)$. For the values, the input parameters appearing in the sum rules are [31,36–38]

$$\begin{aligned} m_c(\bar{m}_c) &= (1.275 \pm 0.025)\ \text{GeV}, \\ m_b(\bar{m}_b) &= (4.18 \pm 0.03)\ \text{GeV}, \\ f_{3\gamma} &= -0.0039\ \text{GeV}^2, \\ \chi &= (3.15 \pm 0.10)\ \text{GeV}^2, \\ \langle \bar{q}q \rangle &= (-0.24 \pm 0.001)^3\ \text{GeV}^3, \\ m_0^2 &= (0.8 \pm 0.2)\ \text{GeV}^2. \end{aligned}$$

For the heavy quark masses, we have used their $\overline{\text{MS}}$ Scheme values. The masses of the spin-3/2 doubly heavy baryons and spin-1/2 doubly heavy baryons are calculated in [20,21,39], and the mass of Ξ_{cc} baryon is experimentally observed. We present the masses in Table II.

We will see that the radiative decay widths of spin-3/2 to spin-1/2 baryons are proportional to the cube of the mass difference of the initial and final baryons, $(\Delta m) = (m_{3/2} - m_{1/2})$. Therefore, the decay widths are very sensitive to the mass difference of doubly heavy baryons. For this reason, in the next discussion, we will use the mass of doubly heavy baryons obtained from lattice calculations which contain a minimal error. The photon distribution amplitudes are the main nonperturbative inputs of light cone sum rules. The expression of DAs and the values of the parameters entering in the expressions of DAs are given in [31]. Now, let us perform the numerical analysis of the relevant form factors.

The sum rules for the transition form factors $G_1(0)$ and $G_2(0)$ involve three auxiliary parameters: parameter β appearing in the expression of the interpolating current for spin-1/2 doubly heavy baryons, the continuum threshold

TABLE II. Baryon masses.

Baryon	Lattice [39]	QCDSR [20]	QCDSR [21]	Experiment [1]	Experiment [2]
Ξ_{bc}	6.943 GeV	6.72 GeV	⋯	⋯	⋯
Ξ'_{bc}	6.959 GeV	6.79 GeV	⋯	⋯	⋯
Ξ_{bb}	10.143 GeV	9.96 GeV	⋯	⋯	⋯
Ξ_{cc}	3.610 GeV	3.72 GeV	⋯	3.52 GeV	3.62 GeV
Ξ^*_{bc}	6.985 GeV	⋯	7.25 GeV	⋯	⋯
Ξ^*_{cc}	3.692 GeV	⋯	3.69 GeV	⋯	⋯
Ξ^*_{bb}	10.178 GeV	⋯	10.4 GeV	⋯	⋯

TABLE III. Working Regions for M^2, β, and s_0.

Transition	M^2	$\cos(\theta)$	s_0
$\Xi_{bc}^{+} \to \Xi_{bc}^{*+}$	6–9 GeV^2	$(-0.4, 0.4)$	57 ± 1 GeV^2
$\Xi_{bc}^{\prime +} \to \Xi_{bc}^{*+}$	6–9 GeV^2	$(-0.4, 0.4)$	57 ± 1 GeV^2
$\Xi_{bc}^{0} \to \Xi_{bc}^{*0}$	6–9 GeV^2	$(-0.4, 0.4)$	57 ± 1 GeV^2
$\Xi_{bc}^{\prime 0} \to \Xi_{bc}^{*0}$	6–9 GeV^2	$(-0.4, 0.4)$	57 ± 1 GeV^2
$\Xi_{cc}^{++} \to \Xi_{cc}^{*++}$	3–6 GeV^2	$(-0.4, 0.4)$	20 ± 1 GeV^2
$\Xi_{cc}^{+} \to \Xi_{cc}^{*+}$	3–6 GeV^2	$(-0.4, 0.4)$	20 ± 1 GeV^2
$\Xi_{bb}^{0} \to \Xi_{bb}^{*0}$	9–12 GeV^2	$(-0.4, 0.4)$	121 ± 2 GeV^2
$\Xi_{bb}^{-} \to \Xi_{bb}^{*-}$	9–12 GeV^2	$(-0.4, 0.4)$	121 ± 2 GeV^2

s_0, and Borel mass parameter M^2. The working region of s_0 is determined from the analysis of two-point sum rules which are carried out in [20,21] and given in Table III.

The working region of M^2 is determined from two requirements. From one side M^2 must be large enough to guarantee the dominance of leading twist over higher twist contributions, and from the other side, it should be small enough in order to ensure the suppression of the higher states and continuum contributions. The working regions of Borel mass parameters are also presented in Table III.

As an example, in Figures 1(a) and 2(a) we present the dependencies of $G_M(0)$ and $G_E(0)$ on M^2 at fixed values of s_0 at β. From these figures, we see that the form factors G_M

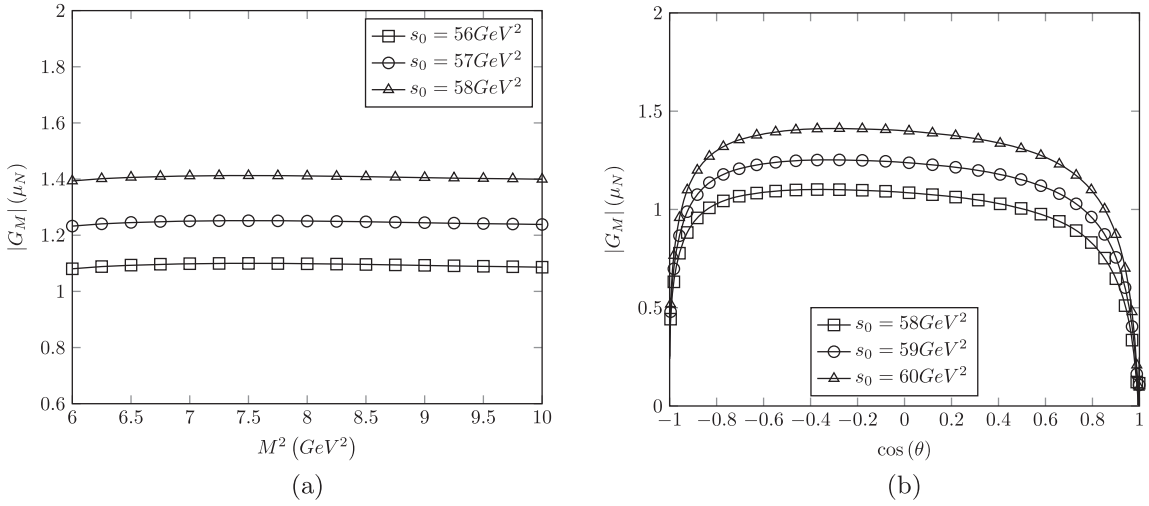

FIG. 1. (a) M^2 dependence of the G_M for $\Xi_{bc}^{*+} \to \Xi_{bc}^{+}\gamma$ decay with different values of s_0 at $\beta = 5$, (b) $\cos(\theta)$ dependence of G_M for $\Xi_{bc}^{*+} \to \Xi_{bc}^{+}\gamma$ with different values of s_0 at $M^2 = 8$ GeV^2, where $\beta = \tan(\theta)$.

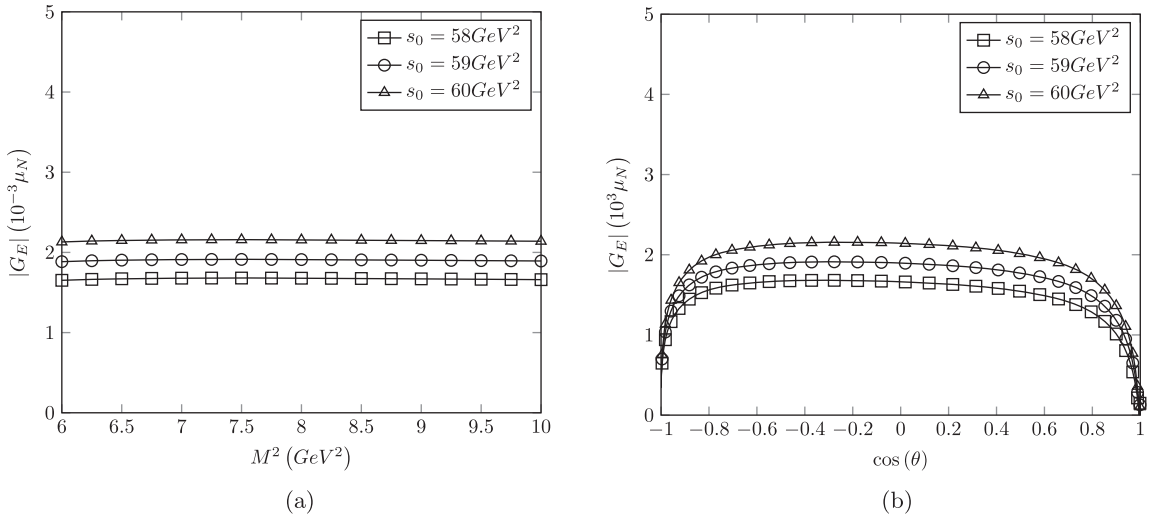

FIG. 2. Same as 1 but for G_E.

TABLE IV. Transition magnetic moments in nuclear magneton.

Transition	This work	QM [23]	χPT [23]	Bag model [24]	EMS [25]	exBag [26]	Lattice [27]
$\Xi_{bc}^{+} \to \Xi_{bc}^{*+}$	1.25 ± 0.156	-1.61	-2.56	0.695	1.12	1.12	⋯
$\Xi_{bc}^{\prime+} \to \Xi_{bc}^{*+}$	0.17 ± 0.030	-0.36	-0.36	0.672	1.04	0.814	⋯
$\Xi_{bc}^{0} \to \Xi_{bc}^{*0}$	0.77 ± 0.104	1.02	1.03	-0.747	-1.03	-0.919	⋯
$\Xi_{bc}^{\prime0} \to \Xi_{bc}^{*0}$	0.18 ± 0.032	-0.36	-0.36	0.070	-0.17	0.598	⋯
$\Xi_{cc}^{++} \to \Xi_{cc}^{*++}$	1.03 ± 0.138	-1.4	-2.35	-0.787	-1.30	-1.21	-0.772
$\Xi_{cc}^{+} \to \Xi_{cc}^{*+}$	0.96 ± 0.158	1.23	1.55	0.945	1.19	1.07	0.906
$\Xi_{bb}^{0} \to \Xi_{bb}^{*0}$	1.78 ± 0.300	-1.82	-2.77	-1.039	-1.70	-1.045	⋯
$\Xi_{bb}^{-} \to \Xi_{bb}^{*-}$	0.82 ± 0.131	0.81	1.13	0.428	0.76	0.643	⋯

TABLE V. Transition electric quadrupole moments in nuclear magneton.

Transition	$\lvert G_E \rvert$
$\Xi_{bc}^{+} \to \Xi_{bc}^{*+}$	$(1.92 \pm 0.239) \times 10^{-3}$
$\Xi_{bc}^{\prime+} \to \Xi_{bc}^{*+}$	$(0.167 \pm 0.029) \times 10^{-3}$
$\Xi_{bc}^{0} \to \Xi_{bc}^{*0}$	$(1.18 \pm 0.160) \times 10^{-3}$
$\Xi_{bc}^{\prime0} \to \Xi_{bc}^{*0}$	$(0.18 \pm 0.032) \times 10^{-3}$
$\Xi_{cc}^{++} \to \Xi_{cc}^{*++}$	$(5.81 \pm 0.775) \times 10^{-3}$
$\Xi_{cc}^{+} \to \Xi_{cc}^{*+}$	$(5.44 \pm 0.901) \times 10^{-3}$
$\Xi_{bb}^{0} \to \Xi_{bb}^{*0}$	$(1.56 \pm 0.264) \times 10^{-3}$
$\Xi_{bb}^{-} \to \Xi_{bb}^{*-}$	$(0.72 \pm 0.115) \times 10^{-3}$

and G_E exhibit excellent stability with respect to the variation of M^2 in its working region.

Finally in order to find the working region of β, we present the dependence of $G_M(0)$ and $G_E(0)$ for the $\Xi_{bc}^{*+} \to \Xi_{bc}^{+}$ transition on $\cos(\theta)$, where $\beta = \tan(\theta)$ in Figures 1(b) and 2(b). From these figures, we see that the results on the form factors show very good stability when $-0.4 < \cos(\theta) < 0.4$. Performing similar calculations for the form factors of other transitions we find that in this region of $\cos(\theta)$ the form factors are rather stable. Therefore the working region of $\cos\theta$ is $(-0.4, 0.4)$.

We performed the numerical analysis by using the working regions of $\cos\theta$, M^2, and s_0, and our final findings of the moments $G_M(0)$ and $G_E(0)$ are collected in Tables IV and V. Note that since the signs of the residues are undetermined, we present the absolute values of our results. All errors coming from uncertainties of input parameters, as well as the variation of s_0, M^2, and $\cos\theta$ in their working regions, are taken quadratically. For comparison in Table IV, we present the predictions for the magnetic moments $G_M(0)$ of other approaches such as quark model [23], χPT [23], bag model [24], effective quark mass scheme [25], extended bag model [26], and lattice QCD [27]. Using the results on the moments G_M and G_E one can easily estimate the decay widths with the help of the following formula:

$$\Gamma = \frac{\alpha}{16} \frac{(m_1^2 - m_2^2)^3}{m_N^2 m_1^3} [G_M^2(0) + 3G_E^2(0)], \tag{22}$$

where m_N is the mass of the nucleon. The results of the decay widths are collected in Table VI.

For completeness, we also presented the decay width results obtained from the bag model, exBag model, RQM, and χPT. We see that our results are drastically different from the results of both approaches, except the results for the $\Xi_{bc}^{*+} \to \Xi_{bc}^{+}\gamma$ and $\Xi_{bc}^{*0} \to \Xi_{bc}^{0}\gamma$ transition

TABLE VI. Decay widths in keV.

Decay	This work	χPT [23]	Bag model [24]	exBag model [26]	RQM [40]	Lattice [27]
$\Xi_{bc}^{*+} \to \Xi_{bc}^{+}\gamma$	0.48 ± 0.119	26.2	0.533	1.31	⋯	⋯
$\Xi_{bc}^{*+} \to \Xi_{bc}^{\prime+}\gamma$	0.002 ± 0.0007	0.52	0.031	0.0293	⋯	⋯
$\Xi_{bc}^{*0} \to \Xi_{bc}^{0}\gamma$	0.18 ± 0.049	7.19	0.612	0.876	⋯	⋯
$\Xi_{bc}^{*0} \to \Xi_{bc}^{\prime0}\gamma$	0.003 ± 0.0009	0.52	0.000	7.6×10^{-5}	⋯	⋯
$\Xi_{cc}^{*++} \to \Xi_{cc}^{++}\gamma$	2.36 ± 0.622	22.0	1.43	2.79	7.21	0.0518
$\Xi_{cc}^{*+} \to \Xi_{cc}^{+}\gamma$	2.07 ± 0.666	9.57	2.08	2.17	3.90	0.0648
$\Xi_{bb}^{*0} \to \Xi_{bb}^{0}\gamma$	0.58 ± 0.188	31.1	0.126	0.137	0.98	⋯
$\Xi_{bb}^{*-} \to \Xi_{bb}^{-}\gamma$	0.12 ± 0.038	5.17	0.022	0.0268	0.21	⋯

obtained from the bag model which are in agreement with our results.

From Table IV we get the following results: Main contributions to the magnetic moments of considered transitions come from the light quarks. In the transitions involving Ξ' the contributions coming from light quarks are canceled. For this reason, the magnetic moment of the transitions involving Ξ' baryons are controlled by heavy quark magnetic moments; hence, they are small. Our calculations confirmed this expectation. Our finding of transition magnetic moments for $\Xi_{bc}^{*+} \to \Xi_{bc}^{+}$, $\Xi_{cc}^{++} \to \Xi_{cc}^{*++}$, $\Xi_{cc}^{+} \to \Xi_{cc}^{*+}$, and $\Xi_{bb}^{*-} \to \Xi_{bb}^{-}$ transitions are in agreement with the QM [23], EMS [25], and exBag [26], but considerably differ from χPT [23]. Results for the $\Xi_{bc}^{*0} \to \Xi_{bc}^{0}$ transition is in agreement with χPT [23] and exBag [26], $\Xi_{bc}^{*0} \to \Xi_{bc}^{\prime 0}$ transition is agreeing with the EMS [25], $\Xi_{bc}^{*0} \to \Xi_{bc}^{0}$ transition is in agreement with bag model [24] and exBag [26], and $\Xi_{bb}^{*0} \to \Xi_{bb}^{0}$ agrees with both QM [23] and EMS [25]. While the results for $\Xi_{cc}^{++} \to \Xi_{cc}^{*++}$ also agree with the quark model [23] and $\Xi_{cc}^{+} \to \Xi_{cc}^{*+}$ agrees with the lattice QCD [27], results for $\Xi_{bc}^{*+} \to \Xi_{bc}^{\prime +}$ transition differs from other approaches' results.

From Table VI we get the following results: The main contribution to the radiative decay widths comes from the transition magnetic moments. In other words, the dominant contributions come from the light quark magnetic moments except the transitions involving Ξ' baryons. The discrepancies among various models are mainly due to the absence of experimental information on the double heavy baryon masses. Any small change in the mass can lead to a considerable change in the decay widths. Our finding of the decay widths for the $\Xi_{bc}^{*+} \to \Xi_{bc}^{+}$ transition is in agreement with the bag model [24], $\Xi_{cc}^{*++} \to \Xi_{cc}^{++}$ and $\Xi_{cc}^{*+} \to \Xi_{cc}^{+}$ are in agreement with the exBag model [26], while $\Xi_{cc}^{*+} \to \Xi_{cc}^{+}$ transition also agrees with the bag model [24]. For other transitions, the results differ from other works.

IV. CONCLUSION

We calculated the magnetic dipole $G_M(0)$ and electric quadrupole $G_E(0)$ form factors of spin-3/2 doubly heavy baryons to spin-1/2 doubly heavy baryon transitions within the light cone sum rules method. Having the values of the magnetic dipole $G_M(q^2)$ and electric quadrupole $G_E(q^2)$ form factors at $q^2 = 0$, we estimate the corresponding decay widths. Our findings on form factors and decay widths compared with the predictions of other approaches.

The difference in predictions of different approaches can be explained as follows:

(1) The choice of the wave function in different models such as NRQM, Hypercentral model, RQM, bag models, etc.
(2) Mixing between $\Xi_{\{bc\}}$ and $\Xi_{[bc]}$ states were ignored in our work.
(3) The transition magnetic moments receive dominant contribution from light quark magnetic moment, and therefore are very sensitive to the screening charge parameter.
(4) Differences in the decay widths can be attributed to the mass splitting of the initial and final baryon states. Due to this reason, different models using different mass splittings have considerably different results. Therefore, the precise determination of the masses of the doubly heavy baryons represents a very important issue for obtaining reliable values of decay widths.

The study of the magnetic moments and decay widths can play an essential role in the determination of the properties of the doubly heavy baryons yet to be observed.

APPENDIX: EXPRESSIONS FOR THE SPECTRAL DENSITIES

Here, we present the expressions for the spectral densities in this study.

1. Spectral densities for symmetric currents

$$\rho_1^S(Q,Q',q) = \frac{3(\beta-1)e_q}{32\sqrt{3}\pi^4}\int_0^1 dx\theta(s-t_{QQ'}(x,\bar{x}))(s-t_{QQ'}(x,\bar{x}))^2 x\bar{x} + \int_0^1 dx\int_0^{1-x} dy\frac{3\theta(s-t_{QQ'}(x,y))}{64\pi^4}$$
$$\times\left\{(\beta-1)(s-t_{QQ'}(x,y))^2[xy\bar{u}_0(2e_q-(e_{Q'}+e_Q))+(e_{Q'}x+e_Qy)]\right.$$
$$-\frac{4m_Qm_{Q'}\beta(s-t_{QQ'}(x,y))}{3xy}(2e_qxy-(1-x-y)(e_{Q'}x+e_Qy))$$
$$\left.+\frac{2(\beta-1)\bar{u}_0(1-x-y)(s-t_{QQ'}(x,y))}{xy}(e_{Q'}m_{Q'}^2x^2+e_Qm_Q^2y^2)\right\}$$

$$
\begin{aligned}
&+\frac{e_q}{48\sqrt{3}\pi^2}\int_0^1 dx\Big\{6\langle\bar{q}q\rangle\bar{u}_0(\beta+1)\int_{u_0}^1 duh_\gamma(u)\rho_{1,1}^{(+)}(s)\\
&-2f_1(\mathcal{A})\frac{f_{3\gamma}(\beta-1)(s-t_{QQ'}(x,\bar{x}))}{(m_Q+m_{Q'})}\rho_{0,0}^{(+)}(s)\frac{(1+3\beta)\langle\bar{q}q\rangle}{48\sqrt{3}\pi^2}\\
&\times\Big[2f_2(\mathcal{T}_4^\gamma)\int_0^1 dx\theta(s-t_{QQ'}(x,\bar{x}))(e_{Q'}m_Q+e_Qm_{Q'})\\
&-f_3(\mathcal{T}_4^\gamma)\int_0^1 dx\theta(s-t_{QQ'}(x,\bar{x}))\frac{e_{Q'}\bar{x}+e_Qx}{x\bar{x}}(m_{Q'}\bar{x}+m_Qx)\Big]\\
&+\frac{\langle\bar{q}q\rangle}{48\sqrt{3}\pi^2}f_3(\mathcal{S}^\gamma)\int_0^1\theta(s-t_{QQ'}(x,\bar{x}))\Big[2\beta(e_Qm_{Q'}+e_{Q'}m_Q)-\frac{(1+\beta)(e_Qm_Qx^2+e_{Q'}m_{Q'}\bar{x}^2}{x\bar{x}}\Big]\\
&+\langle\bar{q}q\rangle[((\beta+1)f_2(4\tilde{\mathcal{S}}+2\mathcal{T}_2+12\mathcal{T}_3-12\mathcal{T}_4)-4f_2(\tilde{\mathcal{S}}+\mathcal{T}_3-\mathcal{T}_4)\\
&-(\beta+1)f_3(3\mathcal{T}_4+3\mathcal{S}+4\mathcal{T}_1+5\mathcal{T}_2+\tilde{\mathcal{S}}))\rho_{0,0}^{(+)}(s)\\
&+(2f_3(2\mathcal{T}_1+\mathcal{T}_3)-(\beta+1)f_3(3\mathcal{T}_3+\tilde{\mathcal{S}}+\mathcal{T}_4-\mathcal{S}-\mathcal{T}_1-\mathcal{T}_2))\rho_{1,0}^{(+)}(s)]\\
&+\frac{3\langle\bar{q}q\rangle(1+3\beta)}{2}(4\chi\varphi_\gamma(u_0)(s-t_{QQ'}(x,\bar{x}))-(2+t_{QQ'}(x,\bar{x}))\mathbb{A}(u_0))\rho_{1,1}^{(+)}(s)\\
&+\frac{f_{3\gamma}}{(m_Q+m_{Q'})}[6\psi^a(u_0)((\beta-1)(3s-2t_{QQ'}(x,\bar{x}))\rho_{0,1}^{(+)}(s)+2\beta m_Qm_{Q'}\rho_{0,0}^{(+)}(s))\\
&+3(\beta-1)(4\psi^v(u_0)-\psi^{a\prime}(u_0))(s-t_{QQ'}(x,\bar{x}))\bar{u}_0\rho_{0,1}^{(+)}(s)]\Big\}
\end{aligned}
\tag{A1}
$$

$$
\begin{aligned}
\rho_2^S(Q,Q',q)=&\int_0^1 dx\int_0^{1-x}dy\frac{3(1-\beta)u_0\bar{u}_0\theta(s-t_{QQ'}(x,y))}{16\sqrt{3}\pi^4}\{(s-t_{QQ'}(x,y))[(1-x-y)(e_{Q'}x+e_Qy)-2xye_q]\}\\
&+\frac{\langle\bar{q}q\rangle(1-\beta)}{12\sqrt{3}\pi^2}f_4(\mathcal{T}_4^\gamma)\int_0^1 dx\delta(s-t_{QQ'}(x,\bar{x})\frac{e_{Q'}m_{Q'}\bar{x}^2+e_Qm_Qx^2}{x\bar{x}}\\
&+\frac{e_q}{24\sqrt{3}}\int_0^1 dx\Big\{\frac{\theta(s-t_{QQ'}(x,\bar{x}))(\beta-1)f_{3\gamma}}{(m_Q+m_{Q'})}\Big[12\int_{u_0}^1 du\bar{u}\psi^v(u)\rho_{0,1}^{(+)}(s)+3u_0\bar{u}_0\psi^a(u_0)\rho_{0,1}^{(+)}(s)\\
&-(f_3-f_2)(\mathcal{A}+\mathcal{V})\rho_{0,0}^{(+)}(s)\Big]+\delta(s-t_{QQ'}(x,\bar{x}))\langle\bar{q}q\rangle\Big[6(1+\beta)\int_{u_0}^1 du\bar{u}(u-u_0)h_\gamma(u)\rho_{1,1}^{(+)}(s)\\
&+2f_4(\mathcal{T}_4-\mathcal{T}_2)(\beta+1)\rho_{0,0}^{(+)}(s)+2f_4(\mathcal{T}_1-\mathcal{T}_3)(\beta-1)\rho_{2,1}^{(+)}(s)\Big]\Big\}
\end{aligned}
\tag{A2}
$$

2. Spectral densities for antisymmetric currents

$$
\begin{aligned}
\rho_1^A(Q,Q',q)=&\frac{1}{32\pi^4}\int_0^1 dx\int_0^{1-x}dy\theta(s-t_{QQ'}(x,y))(s-t_{QQ'}(x,y))\Big\{\frac{1-x-y}{xy}[3(\beta-1)\bar{u}_0(e_Qm_Q^2y^2-e_{Q'}m_{Q'}^2x^2)\\
&-(4\beta+2)m_Qm_{Q'}(e_Qy-e_{Q'}x)]-3(\beta-1)(s-t_{QQ'}(x,y))[xy\bar{u}_0(e_Q-e_{Q'})-(e_Qy-e_{Q'}x)]\Big\}\\
&+\frac{(1-\beta)\langle\bar{q}q\rangle}{144\pi^2}\Big[2f_2(\mathcal{T}_4^\gamma)\int_0^1 dx\theta(s-t_{QQ'}(x,\bar{x}))(e_{Q'}m_Q-e_Qm_{Q'})\\
&-f_3(\mathcal{T}_4^\gamma)\int_0^1 dx\theta(s-t_{QQ'}(x,\bar{x}))\frac{e_{Q'}\bar{x}+e_Qx}{x\bar{x}}(m_Qx-m_{Q'}\bar{x})\Big]
\end{aligned}
$$

$$+\frac{\langle\bar{q}q\rangle}{144\pi^2}f_3(\mathcal{S}^\gamma)\int_0^1\theta(s-t_{QQ'}(x,\bar{x}))\left[6\beta(e_Qm_{Q'}-e_{Q'}m_Q)-\frac{(1+5\beta)(e_Qm_Qx^2-e_{Q'}m_{Q'}\bar{x}^2}{x\bar{x}}\right]$$
$$+\frac{1}{144\pi^2}\int_0^1 dx\left\{\frac{2f_1(\mathcal{V})f_{3\gamma}(\beta-1)(s-t_{QQ'}(x,\bar{x}))}{(m_Q-m_{Q'})}\rho_{0,0}^{(-)}(s)+\langle\bar{q}q\rangle\left[2((\beta-1)f_3(\mathcal{T}_4-\mathcal{T}_3-2\tilde{\mathcal{S}}+\mathcal{T}_2)\right.\right.$$
$$+6f_3(\mathcal{T}_2-\tilde{\mathcal{S}}))\rho_{0,0}^{(-)}(s)+((\beta-1)f_3(\mathcal{T}_2+\mathcal{T}_4+\mathcal{S}-3\tilde{\mathcal{S}})+6f_3(\mathcal{T}_2-\tilde{\mathcal{S}}))\rho_{2,1}^{(-)}(s)$$
$$+((\beta-1)f_3(\mathcal{T}_3-\mathcal{T}_1+4\mathcal{T}_4-6\mathcal{S}+2\tilde{\mathcal{S}}+6\mathcal{T}_2)+6f_3(\mathcal{T}_4-\mathcal{S}+\tilde{\mathcal{S}}-\beta\mathcal{T}_2))\rho_{1,0}^{(-)}(s)$$
$$\left.\left.+\frac{3(1-\beta)}{2}(4(s-t_{QQ'}(x,\bar{x}))\chi\varphi_\gamma(u_0)-(2+t_{QQ'}(x,\bar{x}))\mathbb{A}(u_0))\rho_{1,1}^{(-)}(s)+6\bar{u}_0(\beta+5)\int_{u_0}^1 duh_\gamma(u)\rho_{1,1}^{(-)}(s)\right]\right\} \tag{A3}$$

$$\rho_2^A(Q,Q',q)=\int_0^1 dx\int_0^{1-x}dy\frac{3(\beta-1)u_0\bar{u}_0\delta(s-t_{QQ'}(x,y))}{16\pi^4}[(s-t_{QQ'}(x,y))(1-x-y)(e_{Q'}x-e_Qy)]$$
$$+\frac{\langle\bar{q}q\rangle(1-\beta)}{36\pi^2}f_4(\mathcal{T}_4^\gamma)\int_0^1 dx\delta(s-t_{QQ'}(x,\bar{x})\frac{e_{Q'}m_{Q'}\bar{x}^2-e_Qm_Qx^2}{x\bar{x}}$$
$$\times\frac{e_q}{36\pi^2}\int_0^1 dx\left\{\frac{3(f_2+f_3)(\mathcal{V}+\mathcal{A})f_{3\gamma}(1-\beta)}{2\pi^2(m_Q+m_{Q'})}\theta(s-t_{QQ'}(x,\bar{x}))(x-\bar{x})\rho_{0,0}^{(-)}(s)\right.$$
$$+\delta(s-t_{QQ'}(x,\bar{x}))e_q\langle\bar{q}q\rangle\left[3(\beta+5)\int_0^1 du\bar{u}_0(u-u_0)\theta(u-u_0)h_\gamma(u)\rho_{1,1}^{(-)}(s)\right.$$
$$-f_4((1-v)(\mathcal{T}_4-\mathcal{T}_2))(\beta+5)\rho_{0,0}^{(-)}(s)+\frac{3f_4(\mathcal{T}_1-\mathcal{T}_3)(\beta-1)}{2}\rho_{2,1}^{(-)}(s)$$
$$\left.\left.+f_4(\mathcal{T}_4-\mathcal{T}_2)[(\beta+5)\rho_{2,1}^{(-)}(s)-3(\beta+1)\rho_{1,0}^{(-)}(s)]\right]\right\} \tag{A4}$$

$$\rho_{n,m}^{(\pm)}=\theta(s-t_{QQ'}(x,\bar{x}))(x\bar{x})^m\left(\frac{m_Q}{\bar{x}^n}\pm\frac{m_{Q'}}{x^n}\right) \tag{A5}$$

$$f_1(\varphi)=\int d\alpha_i\frac{\varphi(\alpha_i)}{\alpha_g^2}\theta(u_0-\alpha_{\bar{q}})[\theta(\alpha_g+\alpha_{\bar{q}}-u_0)-\alpha_g\theta(\alpha_g)\delta(\alpha_g+\alpha_{\bar{q}}-u)]$$
$$f_2(\varphi)=\int d\alpha_i\frac{(\alpha_g+\alpha_{\bar{q}}-u_0)\varphi(\alpha_i)\theta(\alpha_g+\alpha_{\bar{q}}-u_0)\theta(u_0-\alpha_{\bar{q}})}{\alpha_g^2}$$
$$f_3(\varphi)=\int d\alpha_i\frac{\varphi(\alpha_i)\theta(\alpha_g+\alpha_{\bar{q}}-u_0)\theta(u_0-\alpha_{\bar{q}})}{\alpha_g}$$
$$f_4(\varphi)=\int d\alpha_i\int_0^1 dv\varphi(\alpha_i)\theta(-v\alpha_g+\alpha_g+\alpha_{\bar{q}}-u_0) \tag{A6}$$

where $t_{QQ'}(x,\bar{x})=\frac{m_Q^2}{\bar{x}}+\frac{m_{Q'}^2}{x}$, $t_{QQ'}(x,y)=\frac{m_Q^2}{x}+\frac{m_{Q'}^2}{y}$.

[1] M. Mattson *et al.* (SELEX Collaboration), Phys. Rev. Lett. **89**, 112001 (2002).

[2] R. Aaij *et al.* (LHCb Collaboration), Phys. Rev. Lett. **119**, 112001 (2017).

[3] R. Aaij *et al.* (LHCb Collaboration), J. High Energy Phys. 12 (2021) 107.

[4] R. Aaij *et al.* (LHCb Collaboration), Sci. China Phys. Mech. Astron. **63**, 221062 (2020).

[5] R. Aaij *et al.* (LHCb Collaboration), J. High Energy Phys. 02 (2020) 049.
[6] V. V. Kiselev and A. K. Likhoded, Phys. Usp. **45**, 455 (2002).
[7] D. Ebert, R. N. Faustov, V. O. Galkin, A. P. Martynenko, and V. A. Saleev, Z. Phys. C **76**, 111 (1997).
[8] S. S. Gershtein, V. V. Kiselev, A. K. Likhoded, and A. I. Onishchenko, Phys. Rev. D **62**, 054021 (2000).
[9] W. Roberts and M. Pervin, Int. J. Mod. Phys. A **23**, 2817 (2008).
[10] F. Giannuzzi, Phys. Rev. D **79**, 094002 (2009).
[11] A. P. Martynenko, Phys. Lett. B **663**, 317 (2008).
[12] A. Valcarce, H. Garcilazo, and J. Vijande, Eur. Phys. J. A **37**, 217 (2008).
[13] Z. Shah and A. K. Rai, Eur. Phys. J. C **77**, 129 (2017).
[14] K.-W. Wei, B. Chen, and X.-H. Guo, Phys. Rev. D **92**, 076008 (2015).
[15] K.-W. Wei, B. Chen, N. Liu, Q.-Q. Wang, and X.-H. Guo, Phys. Rev. D **95**, 116005 (2017).
[16] J.-R. Zhang and M.-Q. Huang, Phys. Rev. D **78**, 094007 (2008).
[17] L. Tang, X.-H. Yuan, C.-F. Qiao, and X.-Q. Li, Commun. Theor. Phys. **57**, 435 (2012).
[18] Z.-G. Wang, Eur. Phys. J. A **45**, 267 (2010).
[19] T. M. Aliev, K. Azizi, and M. Savcı, Phys. Lett. B **715**, 149 (2012).
[20] T. Aliev, K. Azizi, and M. Savcı, Nucl. Phys. **A895**, 59 (2012).
[21] T. M. Aliev, K. Azizi, and M. Savci, J. Phys. G **40**, 065003 (2013).
[22] Q.-F. Lü, K.-L. Wang, L.-Y. Xiao, and X.-H. Zhong, Phys. Rev. D **96**, 114006 (2017).
[23] H.-S. Li, L. Meng, Z.-W. Liu, and S.-L. Zhu, Phys. Lett. B **777**, 169 (2018).
[24] A. Bernotas and V. Šimonis, Phys. Rev. D **87**, 074016 (2013).
[25] A. Hazra, S. Rakshit, and R. Dhir, Phys. Rev. D **104**, 053002 (2021).
[26] V. Simonis, arXiv:1803.01809.
[27] H. Bahtiyar, K. U. Can, G. Erkol, M. Oka, and T. T. Takahashi, Phys. Rev. D **98**, 114505 (2018).
[28] L.-Y. Xiao, K.-L. Wang, Q.-f. Lu, X.-H. Zhong, and S.-L. Zhu, Phys. Rev. D **96**, 094005 (2017).
[29] V. L. Chernyak and I. R. Zhitnitsky, Nucl. Phys. **B345**, 137 (1990).
[30] I. I. Balitsky, V. M. Braun, and A. V. Kolesnichenko, Nucl. Phys. **B312**, 509 (1989).
[31] P. Ball, V. Braun, and N. Kivel, Nucl. Phys. **B649**, 263 (2003).
[32] V. A. Novikov, M. A. Shifman, A. I. Vainshtein, and V. I. Zakharov, Fortschr. Phys. **32**, 585 (1984).
[33] H. Jones and M. Scadron, Ann. Phys. (N.Y.) **81**, 1 (1973).
[34] R. C. E. Devenish, T. S. Eisenschitz, and J. G. Körner, Phys. Rev. D **14**, 3063 (1976).
[35] T. M. Aliev, K. Azizi, and A. Ozpineci, Phys. Rev. D **79**, 056005 (2009).
[36] R. L. Workman *et al.* (Particle Data Group), Prog. Theor. Exp. Phys. **2022**, 083C01 (2022).
[37] V. M. Belyaev and B. L. Ioffe, Sov. Phys. JETP **56**, 493 (1982), http://www.jetp.ras.ru/cgi-bin/e/index/e/56/3/p493?a=list.
[38] M. A. Shifman, A. I. Vainshtein, and V. I. Zakharov, Nucl. Phys. **B147**, 385 (1979).
[39] Z. S. Brown, W. Detmold, S. Meinel, and K. Orginos, Phys. Rev. D **90**, 094507 (2014).
[40] Q.-F. Lü, K.-L. Wang, L.-Y. Xiao, and X.-H. Zhong, Phys. Rev. D **96**, 114006 (2017).